

Ribosomal Elongation Cycle: Energetic, Kinetic and Stereochemical Aspects

Valery I. Lim¹, James F. Curran² and Maria B. Garber^{3*}

¹Engelhardt Institute of Molecular Biology, Russian Academy of Sciences, Vavilov str. 32, 119991 Moscow, Russia

²Department of Biology, Wake Forest University, Winston-Salem, NC 27109, USA

³Institute of Protein Research Russian Academy of Sciences 142290 Pushchino, Moscow Region, Russia

As a preface to an analysis of the ribosomal elongation cycle, we examine the energetics of macromolecular structural transformations. We show that the kinetic barriers and changes of the energetic levels during these transformations are essentially determined by disruption of hydrogen and cation–ligand bonds, and by uncompensated losses of these bonds (ULBs). The disruption of a hydrogen or cation–ligand bond increases the heights of kinetic barriers by the energy of these bonds. The association and dissociation of macromolecules, and conformational transitions within macromolecules, can change the numbers of ULBs but cannot completely eliminate them. Two important general conclusions are drawn from this analysis. First, occupation of enzyme active centers by substrates should be accompanied by a reduction in the number of ULBs. This reduction decreases the activation barriers in enzyme reactions, and is a major contributor to catalysis. Second, the enzymic reactions of the ribosomal cycle (structural changes caused by transpeptidation and by GTP hydrolyses in EF-Tu and EF-G) disrupt kinetic traps that prevent tRNAs from dissociating into solution during their motion within the ribosome and are necessary for progression of the cycle. These results are general purpose structural-functional blocks for building a molecular model of the ribosomal elongation cycle. Here, we demonstrate the utility of these blocks for analysis of acceptance of cognate tRNAs into the ribosomal elongation cycle.

© 2005 Elsevier Ltd. All rights reserved.

Keywords: translation; hydrogen and cation–ligand bonds; kinetic barriers; kinetic traps; ribosomal cycle

*Corresponding author

Introduction

Recent breakthroughs in structural studies of ribosomes and the translational factors^{1–11} provide hope that we will soon understand the entire translational mechanism from initiation through termination in terms of concrete atomic interactions.

Abbreviations used: ULB, ULBs, uncompensated loss(es) of hydrogen and cation–ligand bonds; SREs, steric restriction elements that block the formation of new, compensating hydrogen and cation–ligand bonds in exchange for the disrupted ones; DC, the ribosomal decoding center; DC-SREs, decoding center SREs providing ULBs in wrong decoding complexes; TC, a ternary complex of the aa-tRNA, EF-Tu and GTP; PTC, the peptidyl transferase center.

E-mail address of the corresponding author: garber@vega.protres.ru

The ribosome is a molecular machine in which structural transformations occur during translation.^{12–17} Therefore, to understand the mechanism of translation, in addition to static structures, one must consider the energetic and kinetic aspects of the mechanism; i.e. we must know how and what kinetic barriers and changes of the energetic levels are realized during the structural transformations that occur in the process of translation.

Here, we estimate kinetic barriers and changes of the energetic levels during macromolecular mechanics. Our analysis shows that the kinetic barriers and changes of the energetic levels are basically determined by disruption/formation of hydrogen and cation–ligand bonds, and by uncompensated losses of these bonds. The results obtained are required for building the molecular model of the ribosomal elongation cycle.

Results

Properties of hydrogen and cation–ligand bonds

Property 1. Compared to the other non-covalent interactions hydrogen and cation–ligand bonds possess high sensitivities to their geometrical parameters

In a hydrogen bond, D-H···A-R, a donor group is D-H and an acceptor atom is A. In non-deformed hydrogen bonds the hydrogen, H, is located on the line DA of 2.8–3 Å and steric overlaps of 0.3–0.5 Å between atoms H and A are observed (Figure 1). Because of steric restrictions (Materials and Methods) created by the atom R the angle DAR cannot be less than $\sim 100^\circ$. A deflection of the other angle (the angle DHA) from 180° by only $\sim 30^\circ$ leads to complete disruption of hydrogen bonds.¹⁸ Elimination of a steric overlap between H and A also leads to complete disruption of hydrogen bonds. All of this makes it clear that hydrogen bonds are very sensitive to changes of their geometrical parameters. The same is valid for cation–ligand bonds when the cation is coordinated by ligands. In these cases the cation and its ligands are tightly packed and, therefore, a shift that disrupts one cation–ligand bond almost always disrupts other bonds.

The high sensitivity of hydrogen and cation–ligand bonds to both orientation and distance parameters is their special feature against the background of non-covalent interactions, since those other non-covalent interactions are considerably less sensitive to their geometrical parameters.¹⁹

Property 2. Hydrogen and cation–ligand bonds are relatively high-energy non-covalent interactions

Another special feature of hydrogen and cation–ligand bonds is that they are relatively high-energy non-covalent bonds. Their energy (the enthalpy of disruption of the bond in a vacuum^{18–21}) is $20(\pm 5)$ kJ/mol where ± 5 kJ/mol is the dispersion of the energy of hydrogen and cation–ligand bonds formed by different polar atoms and groups. Energies of $20(\pm 5)$ kJ/mol strongly exceed (by

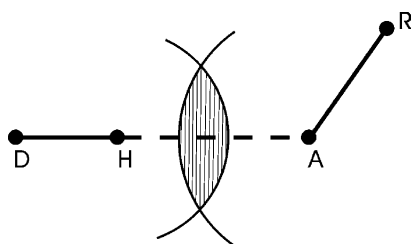


Figure 1. Hydrogen bonding D-H···A-R. D-H is a donor group. A is an acceptor atom forming a covalent bond with an atom R. Arcs demonstrate the van der Waals sizes of atoms H and A. The vertically shaded area is a steric overlap between H and A.

about 1–1.5 orders of magnitude^{18,19}) the energy of the other non-covalent interactions. For example, the van der Waals interaction between different pairs of atoms is about 0.4 kJ/mol while the energy of base stacking determined by a wide diversity of non-covalent interactions is on the order of the thermal energy kT (~ 2.5 kJ/mol). In other words, the energy of one hydrogen or cation–ligand bond in vacuum is equal to the energy of 50 pairs of van der Waals contacts or the stacking between ten bases.

It is important to note, though, that factors of $20(\pm 5)$ kJ/mol are realized only if disrupted hydrogen or cation–ligand bonds are not replaced by bonds to solvent molecules; i.e. the large factor requires that the disrupted bonds are uncompensated losses of hydrogen and cation–ligand bonds.

Uncompensated losses of hydrogen and cation–ligand bonds

Uncompensated losses of hydrogen and cation–ligand bonds (ULBs) arise when for steric reasons new hydrogen and cation–ligand bonds cannot be formed in exchange for the disrupted ones (Materials and Methods). We shall call the atoms and atomic groups that sterically block the formation of new, compensating hydrogen and cation–ligand bonds steric restriction elements or SREs.

Protein and nucleic acid chains as SREs for hydrogen and cation–ligand bonds of solvent molecules interacting with the chains

A water molecule can participate in four hydrogen bonds, sharing its two hydrogen atoms with two acceptors and sharing two further hydrogen atoms associated with two other neighbors. These bonds form a tetrahedrally ordered array in ice whereas liquid water is a disordered network of such hydrogen-bonded molecules.^{22,23} In comparison with solution the possible configurations of hydrogen and cation–ligand bonding created by solvent molecules interacting with protein and nucleic acid chains are sterically restricted by surfaces of these macromolecules. For this reason the solvent molecules in close vicinity of the protein and nucleic acid surfaces can undergo ULBs, i.e. the surfaces of proteins and nucleic acids can play the role of SREs for hydrogen and cation–ligand bonds of the solvent molecules.

The association and dissociation of macromolecules and conformational transitions within macromolecules can change the number of ULBs, but cannot completely eliminate them

The probability of ULBs depends on the distribution of polar atoms on protein and nucleic acid surfaces and the geometry of the surfaces. The density of distribution of polar atoms should be neither very high nor very low (Figure 2(a)), since when the density is high (Figure 2(b)) or low (Figure 2(c)) the interaction of solvent molecules

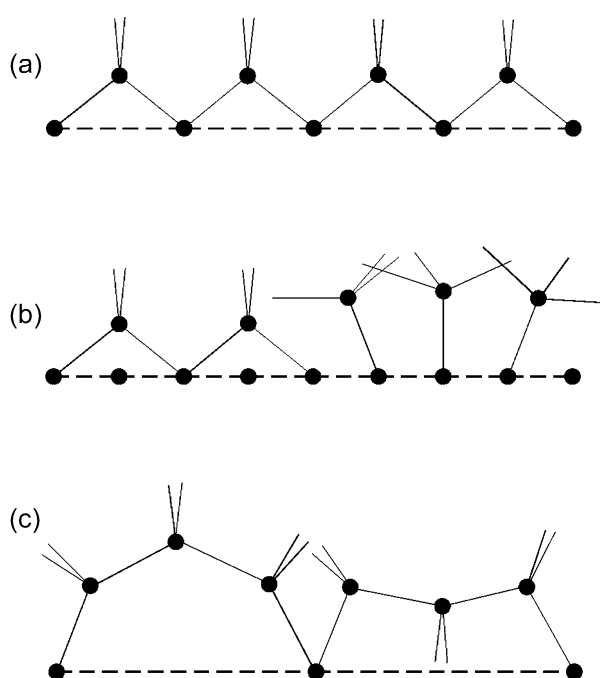


Figure 2. Hydrogen bonding on polar surfaces (one-dimensional case). The broken lines are polar surfaces. Black beads are water molecules and polar atoms of the surfaces. The fine lines are tetrahedrally oriented hydrogen bonds of water molecules. (a) Adjacent polar atoms of the surface form water bridges. (b) Density in distribution of polar atoms on the surface is high. Water molecules cannot form bridges without dehydration of polar atoms on the surface (the left part of the Figure). All polar atoms of a surface form hydrogen bonds with water molecules (right). In this case ULBs are observed on water molecules interacting with polar atoms of a surface. (c) Density in distribution of polar atoms on the surface is low. Water molecules form cavities (left) or they cannot exist without ULBs (right).

with surfaces is impossible without ULBs and cavities. The geometry of the surfaces is also important. It is clear that for steric reasons the probability of ULBs on solvent molecules should increase on concave surfaces and decrease on convex surfaces. This can be demonstrated by transformation of flat surfaces (Figure 2) into concave and convex forms.

The number and sizes of macromolecular surfaces causing ULBs vary with the structural states of macromolecules and their complexes, but they always exist in any structural states including a native state of proteins and nucleic acids. Concave regions (especially in the active center of enzymes), regions without free polar atoms and regions strongly saturated by polar atoms are observed in crystal structures of proteins and nucleic acids. All of this demonstrates that formation and disruption of macromolecular complexes and conformational transitions within macromolecules can change the number of ULBs, but cannot completely eliminate these losses.

Consequences following from properties 1 and 2 of hydrogen and cation–ligand bonds and uncompensated losses of these bonds

Disruption of hydrogen and cation–ligand bonds increases the heights of kinetic barriers by the magnitudes that are a multiple of the energy of hydrogen and cation–ligand bonds

Disruption of a hydrogen or cation–ligand bond is accompanied by an increase in the enthalpy component of the free energy, and this increase ranges up to $20(\pm 5)$ kJ/mol after full disruption of the bond. In principle the enthalpy change during bond disruption can be strengthened or weakened by the entropy changes and by other enthalpy changes. However, a full disruption of a hydrogen or cation–ligand bond is accomplished by shifts of atoms of these bonds of only 0.3–0.5 Å. These minimal atomic shifts do not change 3D structures of molecules significantly; i.e. bond disruption is not accompanied by pronounced changes in the entropy component of the free energy.

The other enthalpy changes are also small against the background of disruption of hydrogen and cation–ligand bonds. The contribution of the other non-covalent interactions can be ignored (property 2) because their energy is small and, moreover, the atomic shifts of 0.3–0.5 Å minimally required for the disruption of hydrogen and cation–ligand bonds are performed without significant disruptions of the other non-covalent interactions. In principle, the kinetic barrier resulting from the disruption of a hydrogen or cation–ligand bond can be decreased by the simultaneous formation of a new hydrogen or cation–ligand bond, but such new bonds are generally impractical for steric reasons. For example, a small deformation of a hydrogen bond can lead to its full disruption (Figure 1 and property 1). Therefore, a hydrogen bond is fully disrupted before it becomes possible for new hydrogen and cation–ligand bonds to form in exchange for the disrupted ones (Materials and Methods). Consequently the free energy increase resulting from the disruption of hydrogen and cation–ligand bonds can be compensated only after their full disruption.

Thus, the disruption of each hydrogen or cation–ligand bond increases the heights of kinetic barriers to conformational changes. The effects of such disrupted bonds on kinetic barriers is additive; therefore, their contribution to kinetic barriers is equal to $N \times 20(\pm 5)$ kJ/mol, where N is the number of hydrogen and cation–ligand bonds that are disrupted simultaneously.

Kinetic barriers counteracting association and dissociation of tRNA–codon complexes from the ribosomal sites

At first glance it would seem that the rigid fixation of one macromolecule onto another can be accomplished with the van der Waals interactions between their surfaces. However, this is not the case

for the following reason. Protein and nucleic acid side-chains on molecular surfaces are often mobile, therefore the rigid fixation of one macromolecule onto another is impossible without inter-molecular hydrogen and cation–ligand bonds. These inter-molecular bonds should not be disrupted and replaced without shifts of one macromolecule relative to the other one. The number of such inter-molecular hydrogen and cation–ligand bonds should be three or more because the rigid fixation of one body onto another requires at least three bonds. It is clear that such inter-molecular hydrogen and cation–ligand bonds should be responsible for the fixation of tRNAs on the ribosomal E, P and A-sites.

Theoretically, three or more hydrogen and cation–ligand bonds that fix tRNAs on the ribosomal sites can be disrupted and replaced sequentially. But sequential disruption requires the rotation of tRNA around one or two tRNA–ribosome hydrogen and/or cation–ligand bonds, and such rotation on the ribosomal surface is unlikely because it will be accompanied by steric overlaps between the tRNA and the ribosome.

In the case of tRNAs in the P and A-sites there is an additional feature that prevents the sequential disruption of the bonds between the ribosomal sites and tRNA–codon complex. This feature is the inter-codon section $-O_{3'}-P-O_{5'}-C_{5'}$ joining the P and A-site duplexes. The mutual orientation of the P and A-site tRNAs in the 70 S ribosome and conformation of the inter-codon section²⁴ are given in Figure 3. Our analysis shows that rotation of either the P-site or A-site tRNA around the bonds of the inter-codon section is accompanied by shifts of the entire P-site or A-site tRNA. This means that all of the bonds between the ribosomal A and P-sites and tRNA–codon complex must be disrupted simultaneously during dissociation of tRNA–codon complexes from the ribosomal sites.

Thus, we should conclude that the hydrogen and cation–ligand bonds that fix tRNA–codon complexes in the ribosomal cycle cannot be disrupted and replaced by others sequentially. Consequently, association and dissociation of tRNA–codon complexes from the ribosomal sites should be confronted by kinetic barriers created by simultaneous formation and disruption of at least three hydrogen and cation–ligand bonds. This means that minimal kinetic barriers counteracting association and dissociation of tRNA–codon complexes from the ribosomal sites should be $3 \times 20(\pm 5)$ kJ/mol.

The average time to overcome kinetic barriers must be less than the average ribosomal cycle time. The times required to overcome barriers imposed by the simultaneous dissociation of three and four hydrogen and/or cation–ligand bonds are several milliseconds and ten seconds (Materials and Methods), respectively. Thus, the time required to overcome kinetic barriers imposed by four bonds exceeds the ribosomal cycle by several orders of magnitude (the average cycle time¹⁰ is $\sim 5 \times 10^{-2}$ s), and therefore the association and dissociation of

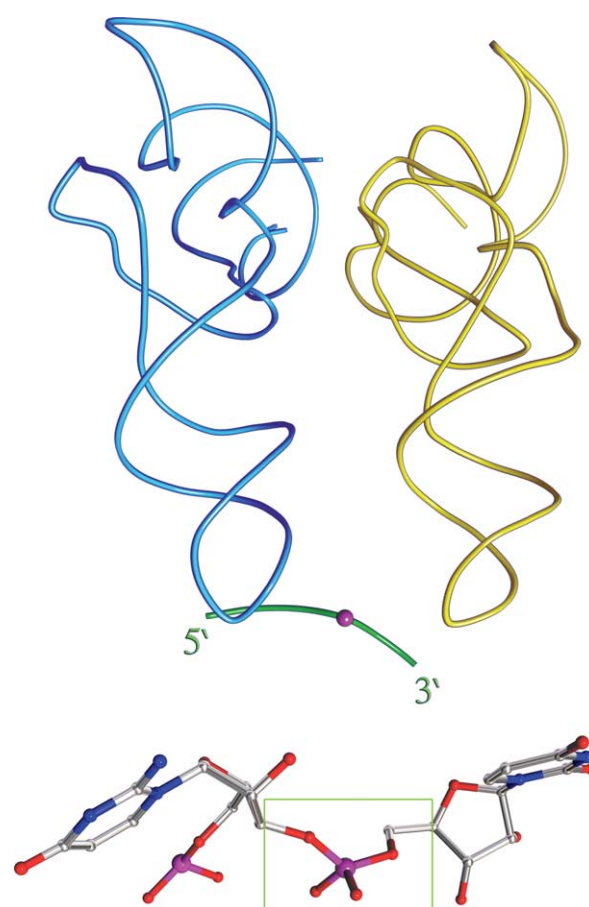


Figure 3. Mutual arrangement²⁴ (PDB1pns.ent) of the tRNAs and mRNA in the P and A-sites. Blue and yellow models are the P and A-site tRNAs, respectively. The CCA ends of the tRNA molecules point away from the reader. The green line is the fragment of mRNA containing the P and A-site codons. The tRNA anticodons are located between the reader and mRNA. The P and A-site codon–anticodon duplexes are not shown. The purple bead on the green line indicates the localization of the inter-codon section $-O_{3'}-P-O_{5'}-C_{5'}$ joining the adjacent duplexes. The conformation of the inter-codon section $-O_{3'}-P-O_{5'}-C_{5'}$ is shown in the rectangle.

tRNA–codon complexes from the ribosomal sites should be confronted by kinetic barriers imposed by three but not four hydrogen and/or cation–ligand bonds. This condition should be fulfilled in the ribosomal cycle when the association or dissociation of tRNA–codon complexes from the ribosomal sites occurs in the absence of GTP hydrolysis and transpeptidation. In the presence of GTP hydrolysis and transpeptidation the fulfillment of this condition is not of necessity, since (see below) these enzyme reactions can decrease kinetic barriers.

Compaction of the protein and nucleic acid chains: the hydrophobic effect

The number of ULBs on polar atoms of protein and nucleic acid chains and on solvent molecules in

the close vicinity of the protein and nucleic acid surfaces depends on the structural state of the chains. On average, the number of ULBs should be reduced, decreasing the surface that is accessible for solvent molecules, since decreasing of such a part of the surface is reducing the number of SREs for solvent molecules. For this reason the protein and nucleic acid chains should tend to compact forms (globular, fibrillar including non-specific aggregation of unfolded chains). Steric restrictions and hydrogen bonding by the polar atoms of protein and nucleic acid chains were used as the primary physico-chemical factors when constructing the classic structures, namely the DNA and RNA double helices, α -helix, β -structures and structures for fibrous proteins.²¹ Perhaps an under-appreciated feature of these structures, however, is that they minimize uncompensated losses of hydrogen and cation–ligand bonds. Importantly, the minimization of ULBs is as important for the stability of structures as the bonding pattern is for determining the specific shape of the low-energy conformation.

One of the SREs for water molecules is massive non-polar side-chains in proteins. When non-polar side-chains are small their action on water molecules is largely entropic and not enthalpic. In this case restriction of the possible configurations of hydrogen and ionic bonding takes place but the overall amount of hydrogen and ionic bonding remains relatively unchanged. However, when a non-polar side-chain is large their surface creates steric hindrances leading to decreasing the overall amount of hydrogen and cation–ligand bonding on solvent molecules interacting with non-polar side-chains. All of this demonstrates that the tendency of solvent molecules located on non-polar surfaces to avoid uncompensated losses of hydrogen bonds should drive the segregation of non-polar side-chains from water solution and lead to the hydrophobic interactions, especially between massive non-polar side-chains.²² A large body of data on 3D structures of proteins and nucleic acids^{18,25} strongly support this. For example, in globular proteins, in contrast to small non-polar side-chains, massive ones as a rule form a hydrophobic core(s) screened from water.

Decreasing the activation barriers in enzyme reactions

In the assembly of substrate–enzyme complexes the substrate–solvent and enzyme–solvent interactions are replaced by substrate–enzyme interactions. By virtue of property 2 of hydrogen and cation–ligand bonds the energetic changes at these replacements should basically be determined by changes in ULBs. Primarily ULBs should be observed on solvent molecules in the active centers of enzymes, since as a rule these centers have a concave form. In other words the active center should contain solvent molecules with ULBs (high-energy solvent molecules). Exclusion of high-energy solvent molecules from the active centers

by correct substrates should be accompanied by reducing the number of ULBs. The energy liberated, thanks to reducing the number of ULBs, can be used for decreasing the activation barriers in enzyme reactions.

As a rule, the activation barriers at enzyme reactions including ribosomal transpeptidation fall in the range 80–120 kJ/mol. In order to obtain the experimentally observed rates of enzyme reactions the activation barriers should be reduced by 20–60 kJ/mol. To do this the binding of substrates to enzymes should distort the low-energy conformation of the attacked grouping into a higher-energy conformation. Importantly, decreases in the number of ULBs can lower activation barriers. For example, energetic losses of 20–60 kJ/mol during transitions from the low-energy conformations to higher-energy substrate conformations can be compensated easily by the exclusion of high-energy solvent molecules from the active centers by substrates.

Kinetic traps in the ribosomal cycle

Definition

As noted above, the lifetimes of structures whose disruption is confronted by the simultaneous breakage of three hydrogen and cation–ligand bonds fit within the typical ribosomal cycle, but those requiring the simultaneous disruption of four or more bonds exceed the ribosomal cycle time by at least three orders of magnitude. It is important that the normal binding and release of tRNAs not be confronted by large barriers, and that their fixation be accomplished by only three hydrogen and/or cation–ligand bonds. It is equally important, however, that tRNAs do not dissociate during intermediate ribosomal stages, such as translocation. Therefore, tRNAs must be trapped kinetically from dissociation during intermediate steps. In other words during the intermediate steps the structures must be formed by tRNAs with the ribosome the disruption of which is confronted by simultaneous breakage of four or more hydrogen and cation–ligand bonds. We will call such structures kinetic traps.

Native structures of proteins and nucleic acids as an example of the kinetic traps

The enthalpic contribution to stability of proteins and nucleic acids comprises hundreds of kJ/mol and it can be obtained only by the elimination of ULBs. Such large contributions are significantly compensated by entropy changes because the entropy of macromolecule chains in the unfolded, random coil state is large. For this reason proteins and nucleic acids are often marginally stable,^{26–29} with a $\Delta G_{\text{folding}}$ value of about -40 kJ/mol to -80 kJ/mol. Consequently, the required stability of proteins and nucleic acids can only be provided kinetically. Let a transition of a protein chain from

an unfolded state to a native be confronted by a kinetic barrier of $3 \times 20 (\pm 5)$ kJ/mol. Such barriers are overcome during co-translational protein folding. Elimination of uncompensated losses of two to three hydrogen and cation–ligand bonds during entry into native structures can lead to the formation of kinetic traps with lifetimes of $10^{4.5}–10^8$ s. This means that a biologically necessary lifetime of native structures of proteins and nucleic acids can be attained by the elimination of uncompensated losses of only two to three hydrogen and cation–ligand bonds.

Disruption of kinetic traps

After performing their functions the kinetic traps should be disrupted. There is the only way to do it: to use structural changes in enzymes caused by exergonic enzyme reactions. In the normal ribosomal cycle the kinetic traps can be disrupted by structural changes caused by transpeptidation and by GTP hydrolyses in EF-G and EF-Tu. In all these enzyme reactions the transformation of substrates into products is accompanied by shifts of the substrate atoms and by changes in stereochemistry of the substrates (Figure 4; transition 1). Because of the action of both these factors hydrogen and cation–ligand bonds will be disrupted but not able to form new ones in the active center. The elimination of these ULBs can remove kinetic traps. There are two general mechanisms for the elimination of ULBs caused by the products of enzymic reactions. One way is for the products to be expelled from the active center and be replaced by solvent molecules (Figure 4; transition 2). Replacement of products of the reaction from the enzyme active center by solvent molecules can disrupt reactant–enzyme kinetic traps.

The other way is a change of the structure of the active center allowing elimination of ULBs caused by shifts of the substrate atoms (Figure 4; transition 3) and by changes in stereochemistry of substrates. A change of the structure of the active centers should be accompanied by rearrangement of the 3D structure of the enzyme, and so the kinetic trap formed by an enzyme molecule with another molecule may be disrupted. A possible example occurs for elongation factor Tu. It is known¹⁰ that the product of GTP hydrolysis, GDP, is held in EF-Tu, and that the structure³⁰ of EF-Tu*GDP is strikingly different^{31,32} from that of EF-Tu with the GTP analogue GDPNP. Whereas the EF-Tu*GTP is compact, the EF-Tu*GDP forms a loose structure with a hole between the domains. It is natural to think that this significant change in 3D structure of EF-Tu is responsible for disruption of the kinetic trap that holds aa-tRNA onto EF-Tu, thus freeing the aa-tRNA for its subsequent interactions with the ribosome.

In conclusion it should be noted that antibiotics and other molecules that affect translation can also disrupt kinetic traps because they may cause rearrangements of kinetic trap hydrogen and cation–ligand bonds.

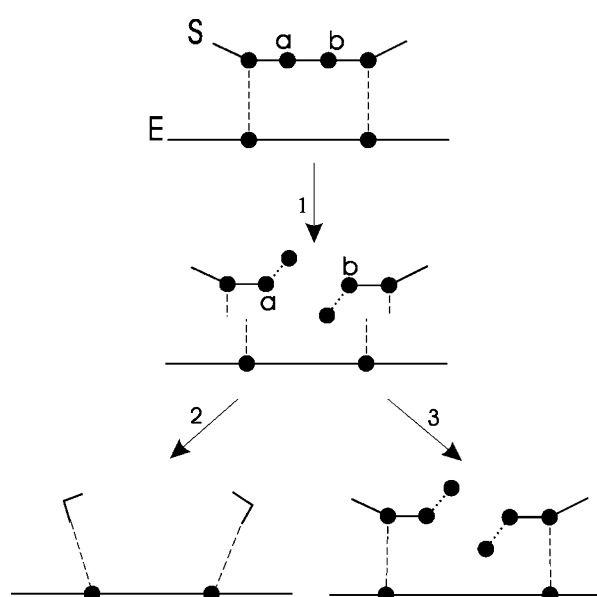


Figure 4. Structural changes caused by the products of an enzyme reaction. S is a substrate; E is the enzyme active center. The broken lines are substrate–enzyme and solvent–enzyme hydrogen and cation–ligand bonds. Transition 1: the substrate into the products of an enzyme reaction. Covalent bond a–b is disrupted and replaced by two new covalent bonds (dotted lines). To avoid a strong steric overlap after disruption of covalent bond a–b the distance ab should be increased by at least 1.4 Å (the difference between the van der Waals contact and the length of a covalent bond). Increasing the distance ab is accompanied by disruption of substrate–enzyme hydrogen and cation–ligand bonds. To avoid uncompensated losses of the disrupted substrate–enzyme hydrogen and cation–ligand bonds the products of an enzyme reaction should be replaced by solvent molecules (transition 2) or the distance between the enzyme polar atoms forming substrate–enzyme hydrogen and cation–ligand bonds should be increased (transition 3).

Acceptance of cognate tRNAs into the ribosomal cycle

The results described above are general purpose structural-functional blocks for building a molecular model for translation. Here, we demonstrate the utility of these blocks for analysis of acceptance of cognate tRNAs into the ribosomal elongation cycle.

Experimental data indicate that the DC and the peptidyl-tRNA duplex co-translocate as a single complex from the A-site to the P-site: why should it occur?

Incorporation of structural information from X-ray crystallography and nuclear magnetic resonance into cryo-electron microscopic maps of ribosomal complexes indicates³³ that elongation factor G actively pushes both the DC and the mRNA–tRNA complex during translocation from the A to the P-site.

The experimental observation described above follows from our kinetic analysis. As noted above, the kinetic barriers confronting association of the tRNA–codon complex with the ribosomal sites are $3 \times 20 (\pm 5)$ kJ/mol. At the same time, the kinetic barriers counteracting formation and disruption of the correct codon–anticodon duplexes are a mere $2 \times 20 (\pm 5)$ kJ/mol. The kinetic barriers of $2 \times 20 (\pm 5)$ kJ/mol are determined by the disruption and formation of two base–base hydrogen bonds.³⁴ In the case of formation and disruption of codon–anticodon duplexes containing G·C pairs the kinetic barrier of $2 \times 20 (\pm 5)$ kJ/mol is provided by the formation of the large propeller twist in G·C pairs. In this case one base–base hydrogen bond is replaced during the twist and the other two by removal of a codon base from the mini helix.³⁴

Thus, we see that the kinetic barriers confronting association of the tRNA–codon complex with the ribosomal sites exceeds the kinetic barriers counteracting formation and disruption of the correct codon–anticodon duplexes. This means that unless the duplex is somehow stabilized, it should disrupt and re-form repeatedly during translocation. In other words, without duplex fixation, runs of nucleotides would equilibrate among alternate reading frames. Before translocation³⁴ the action of DC-SREs (A1492 and A1493 of 16 S rRNA) on the codon–anticodon duplex in the A-site increases the kinetic barriers counteracting the duplex disruption from $2 \times 20 (\pm 5)$ kJ/mol to $4 \times 20 (\pm 5)$ kJ/mol. Such a barrier would give a probability of frameshifting during translocation at levels approximating the experimentally observed frameshift error rate³⁵ (10^{-3} – 10^{-4}). Consequently, to avoid frameshifting the action of DC-SREs on the duplex in the A-site should be retained during translocation, i.e. the DC and the peptidyl-tRNA duplex should co-translocate as a single complex from the A-site to the P-site.

DC oscillation model for selection of the correct codon–anticodon duplexes

DC-SREs distinguish³⁶ the correct from wrong decoding complexes. Cognate and near cognate codon–anticodon duplexes cannot be assembled under the influence of DC-SREs within the time of the standard ribosomal cycle because more than three hydrogen bonds must form under these conditions.³⁴ Therefore, duplex assembly should occur outside of the influence of DC-SREs, and then the DC-SREs and the duplex are drawn together to form the (DC-SREs)–(duplex) complex.

After translocation the DC must return from the P-site to the A-site to provide for selection of the correct codon–anticodon duplexes. However, duplex assembly in the A-site must occur outside the influence of DC-SREs to avoid high kinetic barriers.³⁴ All of this suggests that the DC oscillates between the A and P-sites during aa-tRNA selection; i.e. when the A-site is empty, the DC-SREs associate with the P-site duplex. Then, after a duplex assembles in the A-site the DC will move

from the P-site into a position over the preformed A-site duplex to allow for discrimination. Below we demonstrate that this DC oscillation model provides new insights into the acceptance of cognate tRNAs into the ribosomal cycle.

The path of acceptance of aa-tRNAs into the ribosomal cycle

In a ternary complex (TC) the acceptor part of aa-tRNA is bound³⁷ to EF-Tu. The available data^{9,38} (for a review see Wilson *et al.*¹⁰) show that EF-Tu of a TC binds to the large ribosomal subunit in the region of the L7/L12 stalk and the sarcin-ricin loop of 23 S rRNA. This region forms the center that accelerates the GTP hydrolysis in G-domains of elongation factors Tu and G by at least seven orders of magnitude. In response to this acceleration, the average time for GTP hydrolysis in EF-Tu and EF-G becomes $10^{-2.7}$ s and $10^{-2.2}$ s, respectively.³⁹

Acceptance of aa-tRNAs into the ribosomal cycle begins with GTP hydrolysis in EF-Tu and ends with transpeptidation in the PTC. GTP hydrolysis in EF-Tu frees the acceptor part of aa-tRNA, which may then move (Figure 5) from the ribosomal center accelerating GTP hydrolysis to the PTC located near the base of the central protuberance of the large subunit.^{8,40}

Two different structures of the A-site duplex–DC complex should exist during aa-tRNA acceptance. The first structure is formed during selection of the cognate TC and the other forms as the first one rearranges while the aminoacyl arm moves into the PTC.

The existence of two different duplex–DC complexes in the A-site is supported experimentally. Two studies^{36,41} show that the universally conserved residues A1492 and A1493 of the DC

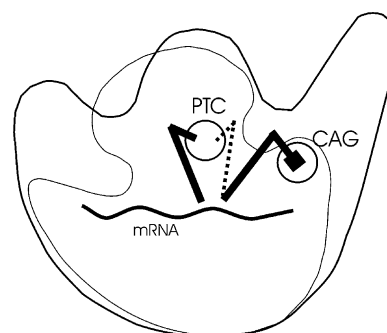


Figure 5. Two positions of aa-tRNA in the ribosome during its inclusion into the ribosomal cycle. The small ribosomal subunit (fine line) is located between the reader and the large subunit. The circles located on the large subunit are PTC and the ribosomal center accelerating the GTP hydrolysis (CAG). Bold lines indicate peptidyl-tRNA located in the P-site and aa-tRNA in the ternary complex. Black square indicates EF-Tu that interacts with the CAG. Broken lines indicate aa-tRNA after a shift of its acceptor part from the CAG to the PTC. The anticodon stems of tRNAs together with mRNA are located on the small subunit.

interact with the codon moiety of duplexes. But, the interactions revealed by these two studies are different.

GTP hydrolysis in a ternary complex should be controlled by DC oscillation: GTP hydrolysis is prohibited when the DC is in P-site position and allowed when the DC is in A-site position

GTP hydrolysis in EF-Tu is triggered by formation of cognate DC-codon-anticodon complexes. Theoretically, in this case two different variants of triggering GTP hydrolysis are possible. One of them is a ternary complex (TC), which binds to the ribosome, and either dissociates or undergoes GTP hydrolysis depending on the stability of codon-anticodon duplexes in the DC-codon-anticodon complexes. By virtue of the low stability of codon-anticodon duplexes non-cognate TCs should dissociate from the ribosome faster than GTP hydrolyses. In contrast, high duplex stability of cognate TCs will generally result in the TC remaining on the ribosome long enough for GTP hydrolysis to occur. The other variant of triggering GTP hydrolysis is that GTP hydrolysis is controlled by interactions of DC with codon-anticodon duplexes.

The variant in which GTP hydrolysis is controlled by duplex stability is unlikely. Bacterial ribosomes stalled on defective mRNAs missing a stop codon are rescued by transfer-messenger RNA (tmRNA), which functions as both tRNA and mRNA. The first ribosomal elongation cycle on tmRNA is highly unusual, in that tmRNA contains a codon mimic but has no anticodon analog,^{42,43} and yet tmRNA triggers GTP hydrolysis. This indicates that the determining role in triggering GTP hydrolysis should belong to the interaction of codon-anticodon duplexes (their codon moiety⁴³) with the ribosomal decoding center. Let us consider this point in detail.

In contrast to cognate (DC-SREs)-(duplex) complexes, the formation of all non-cognate (DC-SREs)-(duplex) complexes is accompanied by an uncompensated loss of at least one hydrogen or cation-ligand bond.³⁴ Therefore, the kinetic barrier counteracting the transition of the DC from the cognate duplex to the P-site position will exceed by at least $20(\pm 5)$ kJ/mol, the kinetic barrier at transition of the DC from non-cognate duplex to the P-site (Figure 6). For this reason the lifetime of the DC in the A-site position with cognate complexes will be increased by three to four orders or more relative to those for near-cognate TCs. This property of the DC provides differences of three to four orders or more in the probability of GTP hydrolysis in cognate and near-cognate TCs if the following two requirements are fulfilled. First, the ribosomal center accelerating GTP hydrolysis should be activated when the DC is in the A-site position and inactivated in the presence of the DC in the P-site position. Second, the lifetime of the DC in the A-site with correct duplexes should not

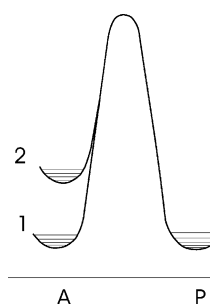


Figure 6. Kinetic barriers between the A and P-site positions of the DC. Curves 1 and 2 represent the kinetic barriers when the A-site is occupied by the cognate and near-cognate codon-anticodon duplexes, respectively. The energetic difference between curves 1 and 2 in the A-site position is $20(\pm 5)$ kJ/mol. Horizontal lines represent energetic levels of the DC at different cognate and near-cognate duplexes in the A and P-sites.

exceed the time ($10^{-2.7}$ s) of GTP hydrolysis by EF-Tu on the ribosome, i.e. the kinetic barriers counteracting the transition of DC from the cognate duplex to the P-site position should be less than or equal to $3 \times 20(\pm 5)$ kJ/mol. Otherwise the transition of DC from near-cognate duplexes to the P-site position will be confronted by the barriers of $3 \times 20(\pm 5)$ kJ/mol or more (Figure 6). The overcoming time of the barrier of $3 \times 20(\pm 5)$ kJ/mol is $10^{-2.5}$ s (Materials and Methods). This time is close to the time ($10^{-2.7}$ s) of GTP hydrolysis by EF-Tu on the ribosome, i.e. GTP hydrolysis in near-cognate TCs will take place.

Activation/inactivation of the ribosomal center accelerating GTP hydrolysis during DC oscillation should be performed by conformational changes in the ribosomal center accelerating GTP hydrolysis. These changes caused by DC oscillation are consistent with experimental data. Rearrangement of the ribosomal center accelerating GTP hydrolysis should be observed during ribosomal translocation, because the DC should be translocated simultaneously with a newly formed peptidyl-tRNA from the A-site to the P-site. Three-dimensional cryo-electron microscopy maps of the 70 S ribosome in various functional states⁴⁴ show that strong conformational changes occur during translocation in the region of the ribosomal center accelerating GTP hydrolysis. One of the most prominent is the bifurcation of the L7/L12 stalk.

DC oscillation and codon context effects

Translation of the codon can depend on adjacent nucleotides (codon context effects; for a review, see Yarus & Curran⁴⁵). By using the measured distance between the P and A-site tRNAs and the crystallographic tRNA structure, Smith & Yarus⁴⁶ proposed a model for the tRNA-tRNA-mRNA complex that should be observed at the moment of transpeptidation when the CCA ends of tRNAs are drawn

together. The anticodon–anticodon contacts in the complex are observed that depend on the wobble base-pair of the P-site duplex. They have been proposed by Smith & Yarus⁴⁶ as one source of codon context effects on aa-tRNA selection.

Another source of codon context effects on the selection of cognate TCs (at this early step the CCA ends of tRNAs are not drawn together; Figure 5) takes place within the framework of the DC oscillation model. The barrier heights in the A and P-site positions of the DC (Figure 6) depend on interactions of the DC with the P and A-site codons. Energy changes caused by these interactions are small in comparison with the energy changes that take place at uncompensated losses of hydrogen and cation–ligand bonds. However, they affect the rate of codon reading in the A-site, i.e. context effects will take place. Thus, the exchange reaction between the P and A-site codons through DC oscillation should provide a wide variety of context effects at the stage of selection of cognate TCs.

About half of cognate aa-tRNAs are expelled from the ribosome on the way to the PTC

GTP hydrolysis by a TC liberates the acceptor part of a cognate aa-tRNA, which is then free to undergo a significant shift towards the PTC (Figure 5). During this shift the codon–anticodon duplex of aa-tRNA anchors it, preventing expulsion of the aa-tRNA from the ribosome. Therefore, the kinetic barriers counteracting the duplex disruption should not be significantly less than the barriers that should be overcome at the shift of aa-tRNA–codon complex to the PTC.

The interaction of cognate codon–anticodon duplexes with the DC strongly increases (to $4 \times 20 (\pm 5)$ kJ/mol) the kinetic barriers counteracting the duplex disruption.³⁴ This means that the lifetime of cognate duplexes is determined by the kinetic barrier counteracting the transition of the DC from the A-site position to the P-site position. As noted above this barrier should be less than or equal to $3 \times 20 (\pm 5)$ kJ/mol. Consequently, the kinetic barriers preventing the expelling of aa-tRNA from the ribosome at its shift to the PTC should not exceed $3 \times 20 (\pm 5)$ kJ/mol.

As to the kinetic barriers that should be overcome at the shift of the aa-tRNA–codon complex to the PTC, they should be $3 \times 20 (\pm 5)$ kJ/mol. Thus, we see that the kinetic barriers preventing the expulsion of aa-tRNA from the ribosome should be about equal to the barriers that should be overcome during the shift of the acceptor part of aa-tRNA to the PTC. This means that the average lifetime of the codon–anticodon duplex should be about equal to the average time of movement of aa-tRNA to the PTC. In this case the probability of aa-tRNA to be involved in the ribosomal cycle after GTP hydrolysis in EF-Tu will be about 0.5 and not 1. Consequently, about half of cognate tRNAs are

lost at this step; therefore, ribosomes require an average of two GTP hydrolyses with two cognate TCs to accept one in the ribosomal cycle. This consequence of our model is supported by experimental data showing that EF-Tu hydrolyzes two GTP molecules in the ribosomal cycle.⁴⁷ This requirement for two GTPs per cognate selection seems wasteful. However, this situation provides an opportunity for proofreading.

Proofreading

Besides the expelling of about half of cognate aa-tRNAs from the ribosome as it shifts towards the PTC, non-cognate tRNAs should also be expelled in this step. And, because of the difference in stability of cognate and non-cognate duplexes the disruption of non-cognate duplexes should be confronted by kinetic barriers that are well under $3 \times 20 (\pm 5)$ kJ/mol, i.e. in accordance with the difference in stability of cognate and non-cognate duplexes the probability of expelling non-cognate tRNAs should greatly exceed 0.5. This means that the movement of aa-tRNA to the PTC after GTP hydrolysis can be considered as a proofreading step at selection of cognate tRNAs.

The fidelity of aa-tRNA selection is determined by initial selection before and proofreading after GTP hydrolysis by EF-Tu. The current concept^{48,49} is that the cognate codon–anticodon, more efficient than the near-cognate one, induces a particular conformation of the decoding center of 16 S rRNA, which in turn promotes GTPase activation and A-site accommodation of aa-tRNA. It is easy to see that our mechanism of aa-tRNA selection is in line with this concept.

Discussion

The main result of this work is a demonstration that the formation and disruption of hydrogen and cation–ligand bonds should play the determining role in the formation and function of protein and nucleic acid structures. The disruption and formation of hydrogen and cation–ligand bonds, disrupted but uncompensated bonds (ULBs), and the elimination of ULBs can be modeled successfully with modern computer graphics equipment³⁴ and, therefore, a kinetic analysis of basic processes in protein and nucleic acids at structural stereochemical level is possible. This is of fundamental importance, since it is unlikely that molecular biological processes and, in particular, the ribosomal cycle^{13,48,49} operate at equilibrium. The results presented here are general purpose structural-functional blocks for building molecular models of various biochemical processes. This consideration of aa-tRNA selection demonstrates the utility of these blocks for the analysis of translation.

Materials and Methods

Calculation of the average time required to overcome energetic barriers

The average time (τ) required to overcome a barrier with the height H is equal to $h/kT \times \exp(H/RT)$. At $T=300$ K, the value of h/kT is about 10^{-13} s. At $H=2 \times 20$ kJ/mol, 3×20 kJ/mol, 4×20 kJ/mol and 5×20 kJ/mol, $\tau=10^{-6}$ s, $10^{-2.5}$ s, 10^1 s and $10^{4.5}$ s, respectively.

Central tenets

A complex was disallowed when at least one interatomic distance was less than the extreme limit (rarely observed steric overlaps⁵⁰). A hydrogen bond D-H...A-R was considered disrupted when HA was greater than or equal to the sum of the van der Waals radii of H and A and/or the angle DHA was less than 150° . For interactions with hydrogen bond donors, anions were considered as hydrogen bond acceptors. Cations with a radius of 1 Å and tetrahedrally oriented bonds were used.

Uncompensated losses of hydrogen and cation–ligand bonds should be caused by steric restriction elements (SREs) counteracting the formation of new hydrogen and cation–ligand bonds in exchange for the disrupted ones

The high sensitivity of hydrogen and cation–ligand bonds to changes of their geometrical parameters allows one to use a great variety of steric restriction elements (SREs) to cause ULBs on both the polar atoms of a macromolecule chain and solvent molecules in the close vicinity of the surface of a macromolecule chain. ULBs can be caused by SREs created by the proper atoms of hydrogen and cation–ligand bonds and by molecular surroundings of polar atoms of the disrupted hydrogen and cation–ligand bonds. For example, a ULB is caused by the proper atom of a hydrogen bond when bond disruption is accomplished by shifts of the atom A (Figure 1) by about 0.5 Å. In this case atom A plays the role of SRE that prohibits the hydrogen bonding of a DH group with a new partner. Another example of SRE is hydrophobic surroundings of hydrogen and cation–ligand bonds. In this case hydrophobic groups will prevent the formation of new hydrogen and cation–ligand bonds in exchange for the disrupted ones (for different type of SREs, see Lim & Curran³⁴).

Acknowledgements

We thank O.S. Nikonov for technical assistance. This work was supported by the Russian Academy of Sciences and the Russian Foundation for Basic Research (02-04-485339), the Council at the RF President (a grant for outstanding scientific schools 1969.2003.4.) and the Program for Molecular and Cellular Biology RAS. The research of M.G. was supported in part by an International Research Scholar's award from the Howard Hughes Medical Institute (grant number 55000308). The work of J.F.C. was supported by NIH grant GM062199.

References

- Liljas, A. & Garber, M. B. (1995). Ribosomal proteins and elongation factors. *Curr. Opin. Struct. Biol.* **5**, 721–727.
- Agrawal, R. K., Penczek, P., Grassucci, R. A. & Frank, J. (1998). Visualization of elongation factor G on the *Escherichia coli* 70S ribosome: the mechanism of translocation. *Proc. Natl Acad. Sci. USA*, **95**, 6134–6138.
- Wilson, K. S. & Noller, H. F. (1998). Mapping the position of translational elongation factor EF-G in the ribosome by directed hydroxyl radical probing. *Cell*, **92**, 131–139.
- Blyn, L. B., Risen, L. M., Griffey, R. H. & Draper, D. E. (2000). The RNA-binding domain of ribosomal protein L11 recognizes an rRNA tertiary structure stabilized by both thiostrepton and magnesium ion. *Nucl. Acids Res.* **28**, 1778–1784.
- Yusupov, M. M., Yusupova, G. Z., Baucom, A., Lieberman, K., Earnest, T. N., Cate, J. H. & Noller, H. F. (2001). Crystal structure of the ribosome at 5.5 Å resolution. *Science*, **292**, 883–896.
- Kisselev, L. L. (2002). Polypeptide release factors in prokaryotes and eukaryotes: same function, different structure. *Structure*, **10**, 8–9.
- Moore, P. B. & Steitz, T. A. (2002). The involvement of RNA in ribosome function. *Nature*, **418**, 229–235.
- Ramakrishnan, V. (2002). Ribosome structure and the mechanism of translation. *Cell*, **108**, 557–572.
- Stark, H., Rodnina, M. V., Wieden, H.-J., Zemlin, F., Wintermeyer, W. & van Heel, M. (2002). Ribosome interactions of aminoacyl-tRNA and elongation factor Tu in the codon-recognition complex. *Nature Struct. Biol.* **9**, 849–854.
- Wilson, D. N., Blaha, G., Connell, S. R., Ivanov, P. V., Jenke, H., Stelzl, U. *et al.* (2002). Protein synthesis at atomic resolution: mechanistics of translation in the light of highly resolved structures for the ribosome. *Curr. Protein Pept. Sci.* **3**, 1–53.
- Bashan, A., Agmon, I., Zarivach, R., Schluenzen, F., Harms, J., Berisio, R. *et al.* (2003). Structural basis of the ribosomal machinery for peptide bond formation, translocation, and nascent chain progression. *Mol. Cell*, **11**, 91–102.
- Woese, C. (1970). Molecular mechanics of translation: a reciprocating ratchet mechanism. *Nature*, **226**, 817–820.
- Rodnina, M. V. & Wintermeyer, W. (2001). Ribosome fidelity: tRNA discrimination, proofreading and induced fit. *Trends Biochem. Sci.* **26**, 124–130.
- Ogle, J. M., Murphy, I. V., Tarry, M. J. & Ramakrishnan, V. (2002). Selection of tRNA by the ribosome requires a transition from an open to a closed form. *Cell*, **111**, 721–732.
- Klaholz, B. P., Pape, T., Zavialov, A. V., Myasnikov, A. G., Orlova, E. V., Vestergaard, B. *et al.* (2003). Structure of the *Escherichia coli* ribosomal termination complex with release factor 2. *Nature*, **421**, 90–94.
- Rawat, U. B. S., Zavialov, A. V., Sengupta, J., Valle, M., Grassucci, R. A., Linde, J. *et al.* (2003). A cryo-electron microscopic study of ribosome-bound termination factor RF2. *Nature*, **421**, 87–90.
- Valle, M., Zavialov, A., Sengupta, J., Rawat, U. & Ehrenberg, M. (2003). Locking and unlocking of ribosomal motions. *Cell*, **114**, 123–134.
- Saenger, W. (1984). *Principles of Nucleic Acid Structure*, Springer, New York.
- Scheraga, H. A. (1968). Calculations of conformations of polypeptides. *Advan. Phys. Org. Chem.* **6**, 103–183.

20. Pauling, L. & Pauling, P. (1975). *Chemistry*, WH Freeman & Company, San-Francisco.
21. Watson, J. D. (1976). *Molecular Biology of the Gene*, WB Benjamin, Inc, Menlo Park, CA.
22. Chandler, D. (2002). Hydrophobicity: two faces of water. *Nature*, **417**, 491.
23. Finney, J. L. (2004). Water? What's so special about it? *Phil. Trans. Roy. Soc. ser. B*, **359**, 1145–1165.
24. Vila-Sunjurjo, A., Ridgeway, W. K., Seyman, V., Zhang, W., Santoso, S., Yu, K. & Cate, J. H. D. (2003). X-ray crystal structure of the wt and a hyper-accurate ribosome from *Escherichia coli*. *Proc. Natl Acad. Sci. USA*, **100**, 8682–8686.
25. Lim, V. I. (1974). Structural principles of the globular organization of protein chains. A stereochemical theory of globular protein secondary structure. *J. Mol. Biol.* **88**, 857–872.
26. Filimonov, V. (1986). The thermodynamics of conformation transitions in polynucleotides. In *Thermodynamic Data for Biochemistry and Biotechnology* (Hinz, H.-J., ed.), pp. 377–401, Springer, Berlin/Heidelberg/New York/Tokyo.
27. Lazaridis, T., Archontis, G. & Karplus, M. (1995). Enthalpic contribution to protein stability: insights from atom-based calculations and statistical mechanics. *Advan. Protein Chem.* **47**, 231–306.
28. Makhatadze, G. I. & Privalov, P. L. (1995). Energetics of protein structure. *Advan. Protein Chem.* **47**, 307–425.
29. Taverna, D. M. & Goldstein, R. A. (2002). Why are proteins marginally stable? *Proteins: Struct. Funct. Genet.* **46**, 105–109.
30. Kjeldgaard, M. & Nyborg, J. (1992). Refined structure of elongation factor Tu from *Escherichia coli*. *J. Mol. Biol.* **223**, 721–742.
31. Berchtold, H., Reshetnikova, L., Reiser, C. O. A., Schirmer, K., Sprinzl, M. & Hilgenfeld, R. (1993). Crystal structure of active elongation factor Tu reveals major domain rearrangements. *Nature*, **365**, 126–132.
32. Kjeldgaard, M., Nissen, P., Thirup, S. & Nyborg, J. (1993). The crystal structure of elongation factor EF-Tu from *Thermus aquaticus* in the GTP conformation. *Structure*, **1**, 35–50.
33. VanLoock, M. S., Agrawal, R. K., Gabashvili, I. S., Qi, L., Frank, J. & Harvey, S. C. (2000). Movement of the decoding region of the 16S ribosomal RNA accompanies tRNA translocation. *J. Mol. Biol.* **304**, 507–515.
34. Lim, V. I. & Curran, J. F. (2001). Analysis of codon:anticodon interactions within the ribosome provides new insights into codon reading and the genetic code structure. *RNA*, **7**, 942–957.
35. Atkins, J. F., Elseviers, D. & Gorini, L. (1972). Low activity of β -galactosidase in frameshift mutants of *Escherichia coli*. *Proc. Natl Acad. Sci. USA*, **69**, 1192–1195.
36. Ogle, J. M., Brodersen, D. E., Clemons, W. M., Jr, Tarry, M. J., Carter, A. P. & Ramakrishnan, V. (2001). Recognition of cognate transfer RNA by the 30S ribosomal subunit. *Science*, **292**, 897–902.
37. Nissen, P., Kjeldgaard, M., Thirup, S., Polekhina, G., Reshetnikova, L., Clark, B. F. C. & Nyborg, J. (1995). Crystal structure of the ternary complex of Phe-tRNA^{Phe}, EF-Tu, and a GTP analog. *Science*, **270**, 1464–1472.
38. Stark, H., Rodnina, M. V., Rinke-Appel, J., Brimacombe, R., Wintermeyer, W. & van Heel, M. (1997). Visualization of elongation factor Tu on the *Escherichia coli* ribosome. *Nature*, **389**, 403–406.
39. Mohr, D., Wintermeyer, W. & Rodnina, M. V. (2002). GTPase activation of elongation factor Tu and G on the ribosome. *Biochemistry*, **41**, 12520–12528.
40. Schmeing, T. M., Seila, A. C., Hansen, J. L., Freeborn, B., Soukup, J. K., Scaringe, S. A. *et al.* (2002). A pre-translocational intermediate in protein synthesis observed in crystal of enzymatically active 50S subunits. *Nature Struct. Biol.* **9**, 225–230.
41. Yoshizawa, S., Fourmy, D. & Puglisi, J. D. (1999). Recognition of the codon-anticodon helix by ribosomal RNA. *Science*, **285**, 1722–1725.
42. Valle, M., Gillet, R., Kaur, S., Henne, A., Ramakrishnan, V. & Frank, J. (2003). Visualizing tmRNA entry into a stalled ribosome. *Science*, **300**, 127–130.
43. Lim, V. I. & Garber, M. B. (2005). Analysis of recognition of transfer-messenger RNA by the ribosomal decoding center. *J. Mol. Biol.* **346**, 395–398.
44. Frank, J. & Agrawal, R. K. (2000). A ratchet-like intersubunit reorganization of the ribosome during translocation. *Nature*, **406**, 318–322.
45. Yarus, M. & Curran, J. F. (1992). The translational context effect. In *Transfer RNA in Protein Synthesis* (Hatfield, D. L., Lee, B. J. & Pirtle, R. M., eds), pp. 319–365, CRC Press, Boca Raton, FL.
46. Smith, D. & Yarus, M. (1989). tRNA-tRNA interactions within cellular ribosomes. *Proc. Natl Acad. Sci. USA*, **86**, 4397–4401.
47. Weijland, A. & Parmeggiani, A. (1994). Why do two EF-Tu molecules act in the elongation cycle of protein biosynthesis? *Trends Biochem. Sci.* **19**, 188–193.
48. Pape, T., Wintermeyer, W. & Rodnina, M. (1999). Induced fit in initial selection and proofreading of aminoacyl-tRNA on the ribosome. *EMBO J.* **18**, 3800–3807.
49. Blanchard, S. C., Gonzalez, R. L., Jr, Kim, H. D., Chu, S. & Puglisi, J. D. (2004). tRNA selection and kinetic proofreading in translation. *Nature Struct. Mol. Biol.* **11**, 1008–1014.
50. Ramachandran, G. N. & Sasisekharan, V. (1968). Conformation of polypeptides and proteins. *Advan. Protein Chem.* **28**, 283–437.

Edited by J. Doudna

(Received 9 February 2005; received in revised form 31 May 2005; accepted 7 June 2005)
Available online 24 June 2005